Supporting information

Design and Synthesis of New Benzimidazole-Carbazole Conjugates for the Stabilization of Human Telomeric DNA, Telomerase Inhibition and their Selective Action on Cancer Cells

Basudeb Maji,[1] Krishan Kumar,[1] Mangesh Kaulage,[1,3] K. Muniyappa[3] and Santanu Bhattacharya[1, 2*]

[1]Department of Organic Chemistry, Indian Institute of Science, Bangalore 560 012, India;

[2]Jawaharlal Nehru Centre for Advanced Scientific Research, Bangalore 560 012, India;

[3]Department of Biochemistry, Indian Institute of Science, Bangalore 560 012, India.

*****To whom correspondence should be addressed.*

E-mail: sb@orgchem.iisc.ernet.in; Phone: (91)-80-2293 2664; Fax: (91)-80-2293 0529

Content **Page**

General. All the starting materials were purchased from the best known commercial sources and were used without further purification. The solvents used in the synthesis, tetrahydrofuran (THF), acetone, dimethylformamide (DMF) etc. were reagent grade and dried prior to use. Thin layer chromatography (TLC) analysis was carried out on silica gel GF 254 precoated glass slides and detected under UV-light or I_2 vapor. For column chromatography, silica gel of mesh size 60-120 and neutral alumina have been used. ^{1}H- and ^{13}C-NMR spectra were recorded using Jeol JNM δ-300 and 400 (300 and 400 MHz for ^{1}H) or Bruker Avance 400 (400 MHz for ^{1}H and 100.577 MHz for ^{13}C) spectrometer and chemical shifts (δ) are reported ppm downfield from the internal standard, TMS. Mass spectra were recorded on a Micromass Q-TOF Micro TM spectrometer.

Synthesis.

4-Cyanoacetanilide (12). 4-Aminobenzonitrile (1.0 g, 9.6 mmol) was dissolved with heating in dil. HCl (1.0 mL of conc. HCl in 9 ml of water). Acetic anhydride (3.7 mL) and sodium acetate (1.2 g in 3.5 g of water) were added to the mixture resulting in a thick white suspension. The mixture was then stirred and cooled in ice for 20 min followed by filtration to afford a white solid which was further recrystallized from ethanol to afford 4-cyanoacetanilide as white crystals (1.37 g, 98 %). ^{1}H NMR (400 MHz, DMSO-d_6) δ ppm 10.39 (s, 1H), 7.76 (s, 4H), 2.10 (s, 3H). mp 206-207 ^{o}C (lit. mp 205-208 ^{o}C).[1]

4-Cyano-2-nitroacetanilide (13). 4-cyanoacetanilide (1.0 g, 6.25 mmol) was added in batches to a solution of KNO_3 (1.35 g, 13.25 mmol) in 6 mL conc. H_2SO_4 and stirred for 1 h maintaining the temperature below 0 ^{o}C. The bright yellow syrup was poured onto ice (25.0 g) and the resulting

precipitate was dried and recrystallized from methanol affording the desired product 4-cyano-2-nitroacetanilide as bright-yellow needles (1 g, 85%). mp 130-131 ^{o}C (lit. mp 131 ^{o}C).[1]

4-Amino-3-nitrobenzonitrile (14). 4-cyano-2-nitroacetanilide (1.0 g, 5.0 mmol) was heated under reflux in 10% H_2SO_4 (65ml) for 30 min and cooled resulting a precipitate which was filtered off and dried. Recrystallization of this material from methanol/water gave yellow crystals of 4-amino-3-nitro benzonitrile (0.7 g, 95%). IR (KBr): 34953471, 3383, 3342, 3186, 3081, 2925, 2228, 1653, 1636, 1600, 1556, 1521, 1356, 1286, 1272, 1203, 1175, 1089, 1021, 919, 829 cm^{-1}; mp 162 ^{o}C (lit. mp 161 ^{o}C).[1]

Ethyl-4-amino-3-nitrobenzene carboximidate hydrochloride (15). Compound 4-amino-3-nitrobenzonitrile (1.0 g, 12.5 mmol) was suspended in dry ethanol (100 ml at 10.0 mg/ml concentration) and cooled over an ice-bath. Anhydrous HCl gas was bubbled rapidly through the mixture for 30-45 min. During this time, solid dissolution followed by rapid precipitation was observed. The vessel was fitted with a $CaCl_2$ drying tube and the thick suspension was stirred overnight and then left for 6-7 days. The ethanol from the reaction mixture was removed under reduced pressure and the pasty residue was triturated with dry diethyl ether. Filtration followed by drying under reduced pressure afforded the imino ether hydrochloride as a hygroscopic bright yellow powder (1.3 g. 85%).

^{1}H NMR (400 MHz, DMSO-d_6) δ ppm 11.44 (br, 2H), 8.80 (s, 1H), 8.36 (s, 2H), 8.14 (d, J = 9.2, 1H), 7.17 (d, J = 9.2, 1H), 4.58 (q, J = 6.8, 2H), 1.46 (t, J = 6.8, 3H); mp 233 ^{o}C (lit. mp 233-234 ^{o}C).[35]

4-[5'-(4'-Methylpiperazin-1'-yl)benzimidazol-2'-yl]-2-nitroaniline (16). A mixture of freshly prepared compound **6** (1 g, 4.85 mmol) and compound **15** (1.19 g, 4.85 mmol) in dry ethanol/ glacial acetic acid (2:1, 69 ml) was refluxed for 4 h under nitrogen. The mixture was cooled and

then concentrated to afford an orange pasty residue. This material was then dissolved in water and addition of conc. ammonia solution to it resulted in precipitation of a solid. The suspension was allowed to stand overnight. This resulted in the complete sedimentation of a brick red solid which was collected by filtration and washed thoroughly with water before being dissolved in acetic acid/methanol (7.5: 92.5, 25 mL). The deep red solution was filtered and then made alkaline with conc. ammonia solution (25%, 20 ml). A fine orange precipitate formed immediately and the suspension was allowed to stand for several hours before filtration. The solid thus retained was washed thoroughly with water and then with acetone. Drying under reduced pressure afforded the pure an orange solid product (1.33 g, 78%).

^{1}H NMR (400 MHz, DMSO-d_6) δ ppm 12.60 (br, 1H), 8.74 (s, 1H), 8.14 (d, J = 8.4, 2H), 7.76 (s, 2H), 7.43 (s, 1H), 7.13 (d, J = 8.4, 1H), 6.92 (s, 2H), 3.12 (s, 4H), 2.54 (s, 4H), 2.27 (s, 3H); mp 184-186 ^{o}C (lit. mp 183-184 ^{o}C).[1]

2-Amino-4-[5'-(4"-methylpiperazin-1"-yl)benzimidazol-2'-yl]aniline (17). A solution of 4-[5'-(4"-methylpiperazin-1"-yl)benzimidazol-2'-yl]-2-nitroaniline **(16)** (1.04 g, 3.0 mmol) in absolute ethanol was treated with 10% palladium on carbon (300 mg) and hydrogenated at rt for 36 h. The solution was then filtered through a bed of celite and concentrated under reduced pressure affording the orange-brown colored diamine **17** (0.966 g, 100%) and used for the next reaction without any further purification as the diamine product was found to be highly unstable.

UV-Vis titration of the ligands with preformed G-quadruplex DNA.

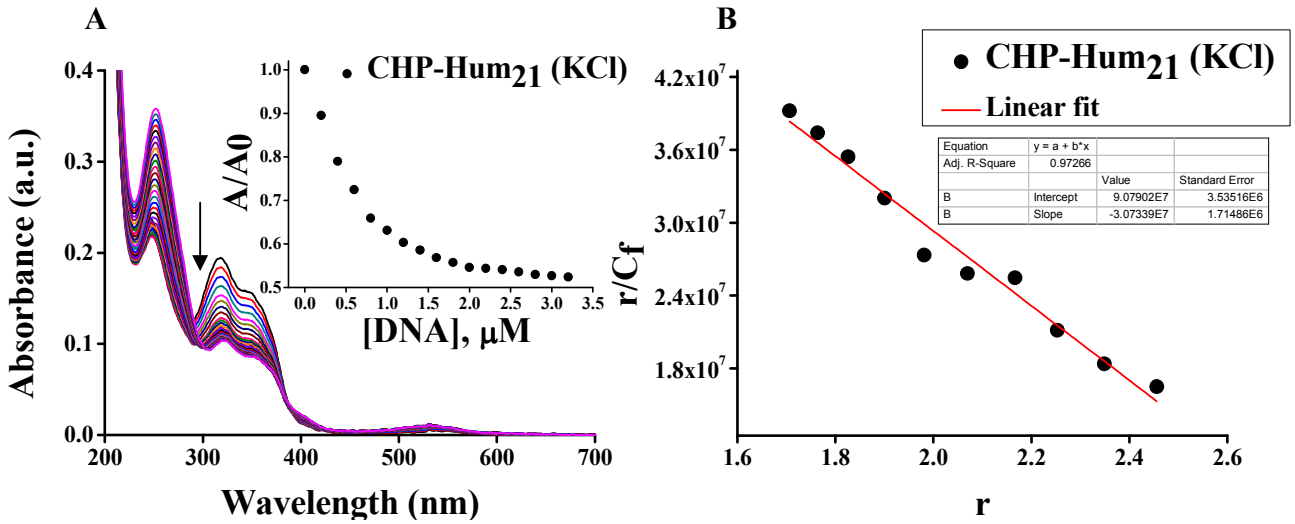

Figure S1. UV-Vis titration of 5 μM **CHP** with (A) Hum_{21} G-quadruplex DNA in Tris-HCl (pH 7.4), having 0.1 M KCl and 0.1 mM EDTA and (B) the corresponding scatchard plot.

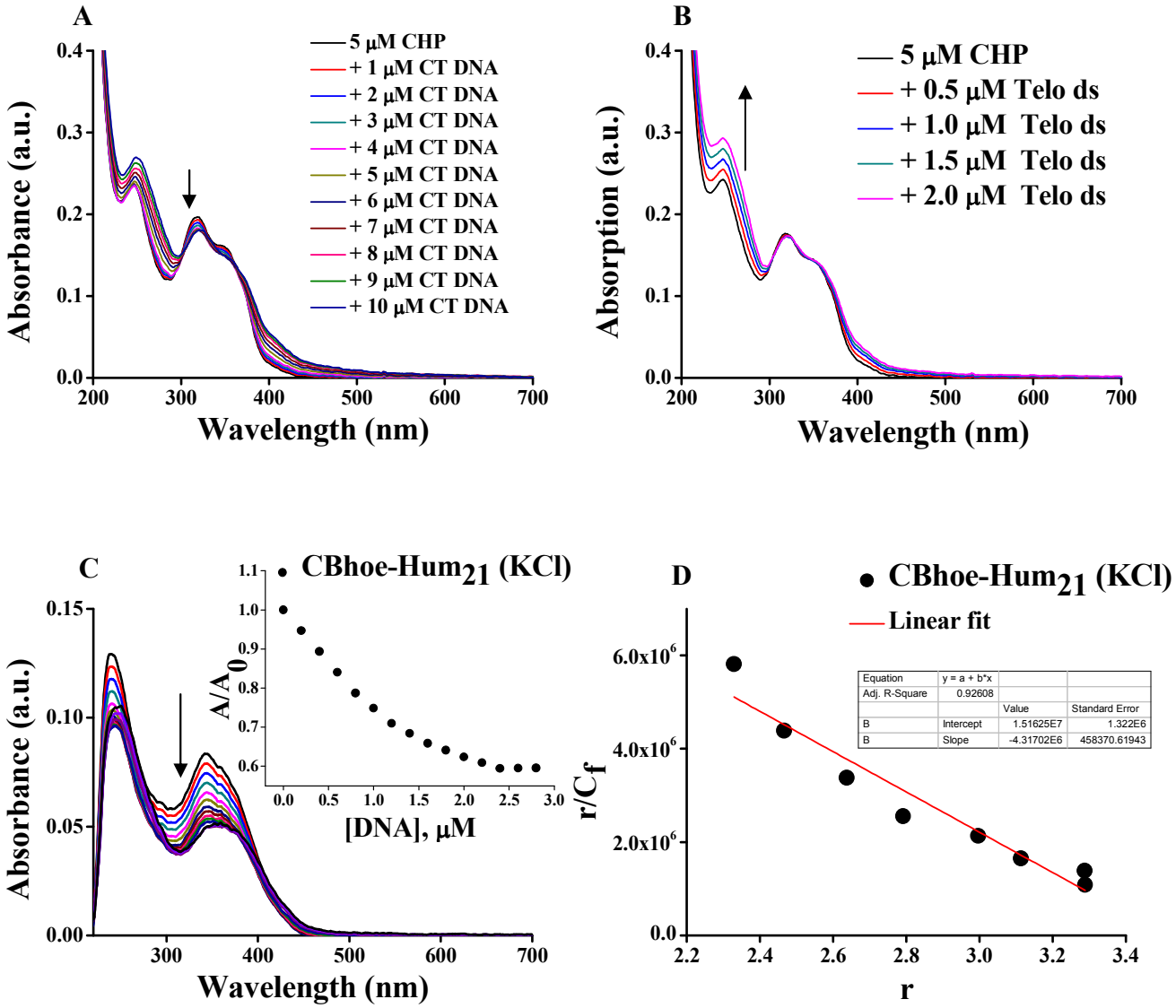

Figure S2. UV-Vis titration of 5 μM **CHP** in presence of (A) CT DNA in Tris-HCl (pH 7.4), having 40 mM NaCl and 0.1 mM EDTA and (B) telomeric duplex d[5′-$G_3(T_2AG_3)_3$-3′]/[5′-$(C_3TA_2)_3C_3$-3′] in Tris-HCl (pH 7.4), having 40 mM NaCl and 0.1 mM EDTA. (C) UV-Vis titration of 5 μM **CBhoe** with Hum_{21} G-quadruplex DNA in Tris-HCl (pH 7.4), having 0.1 M KCl and 0.1 mM EDTA and (D) the corresponding scatchard plot.

The binding constants were calculated from the linear Scatchard equation which has been discussed in the supporting information and this is reproduced below. The wavelength in the absorption titration for the calculation of binding constants has been also mentioned in the new

manuscript. The calculation of C_f, C_b and r values is presented in the supporting information and briefly mentioned below.

$$r/C_f = K_a(n - r) \quad \text{.....1}$$

Table S1. Calculation for Scatchard plot.

A_{free} 0.084		A_{sat} 0.05005	C = [Ligand] 0.000005 (M)		x-axis	y-axis
A_t	$\alpha = (Afree-At)/(A_0-A_{sat})$	1- α	$C_f = (1-\alpha) \times$ [Ligand] (M)	[DNA] (μM)	$r = (C-C_f) \times 10^6/[DNA]$	$r/C_f (M^{-1})$
0.07954	0.131	0.869	4.3E-06	0.2	3.28	756188.5
0.07507	0.263	0.737	3.7E-06	0.4	3.29	892286.2
0.07061	0.394	0.606	3.0E-06	0.6	3.29	1085441
0.06614	0.526	0.474	2.4E-06	0.8	3.29	1387508
0.06286	0.62	0.38	1.9E-06	1	3.11	1650273
0.05958	0.719	0.281	1.4E-06	1.2	2.99	2135362
0.05746	0.782	0.218	1.1E-06	1.4	2.79	2558319
0.05534	0.844	0.156	7.8E-07	1.6	2.64	3386106
0.05386	0.888	0.112	5.6E-07	1.8	2.47	4394867
0.05237	0.932	0.068	3.4E-07	2	2.33	6816810
0.05116	0.967	0.033	1.6E-07	2.2	2.20	13447993
0.05005	1	0	0	2.8	1.79	---

Binding assays were performed with pre-formed d[5′-$G_3(T_2AG_3)_3$-3′] quadruplex in 10 mM Tris-HCl, having 0.1 M KCl/NaCl and 0.1 mM EDTA buffer, and with d[5′-$G_3(T_2AG_3)_3$-3′]/[5′-$(C_3TA_2)_3C_3$-3′] duplex DNA or CT DNA in 10 mM Tris-HCl, having 40 mM NaCl and 0.1 mM EDTA buffer at pH 7.4. Ligand solution (20 μM/10 μM, 500 μl) was titrated by stepwise addition of aliquots of DNA solution. After each addition, the mixture was incubated at 25 °C for 15 min before measurement. The fractional decrease in absorbance at 320 (for **CMP**, **CHP** and **CBM**) or 340 nm (for **CBhoe**) for each [DNA]/[ligand] ratio was normalized using,

$\Delta A = (A_{free} - A)/(A_{free} - A_{sat})$,

where A_{free} and A_{sat} are the absorbance for the free and fully bound ligands. The fraction of bound drug α (on a 0-1 scale) at each intermediate titration position is given directly by the relative ΔA hypochromicity term.[2] The concentration of free ligand is calculated using

$C_f = (1 - \alpha) \times C$,

where C is the total ligand concentration (fixed at 50 μM) and can be used to determine the binding ratio r, defined as $(C - C_f)$/[DNA]. Titration data were cast into the form of Scatchard plots of r/C_f versus r for analysis where K_a is the intrinsic equilibrium binding constant and n is an exclusion parameter that defines the number of ligand molecules bound per DNA quadruplex. Data were also fitted using the simpler, linear Scatchard equation, **1.**

Additional Fluorescence data.

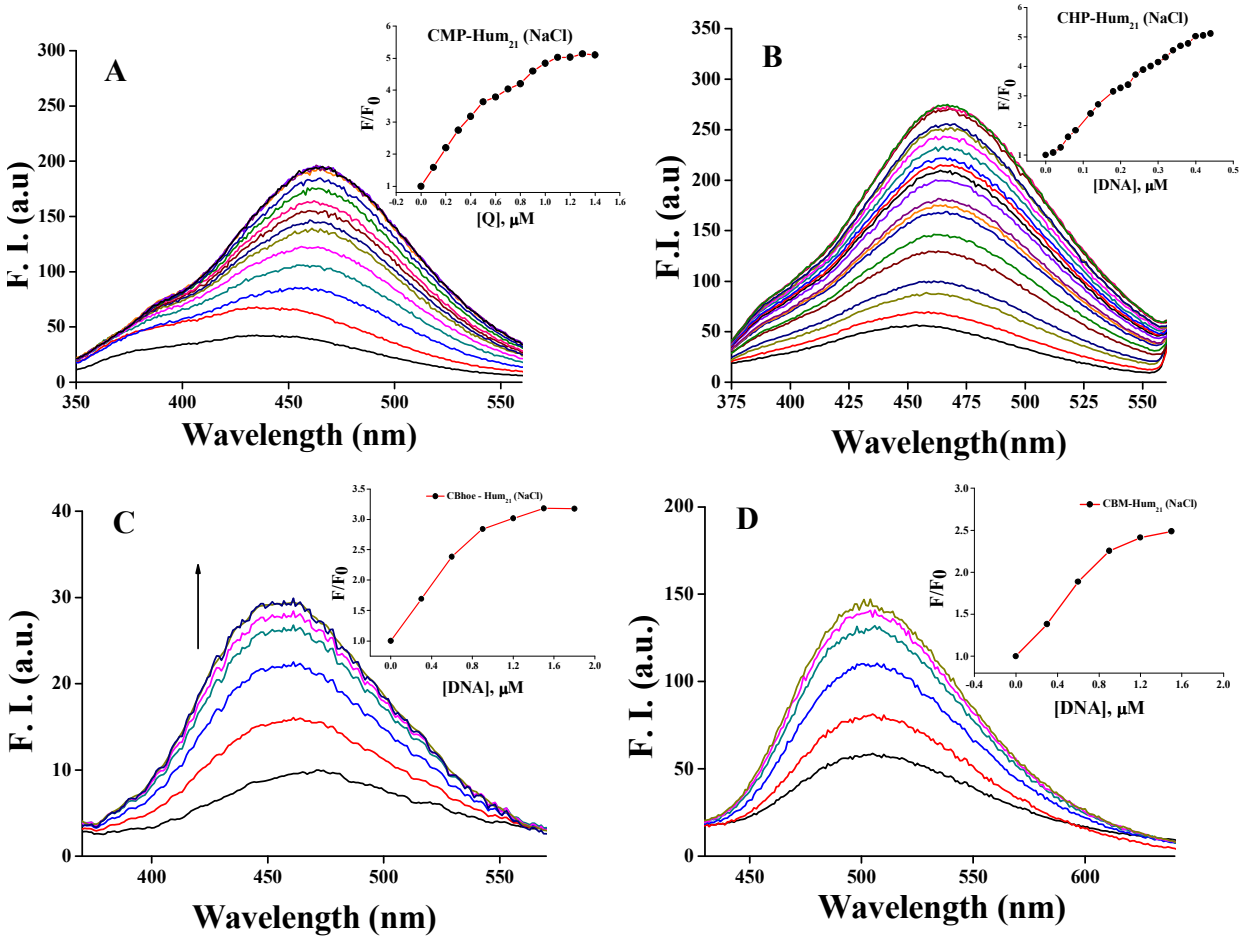

Figure S3. Fluorescence titration of 0.4 μM (A) **CMP**, (B) CHP, (C) **CBhoe** and (D) **CBM** in 10 mM Tris-HCl (pH 7.4) containing 0.1 mM EDTA and 0.1 M NaCl with preformed Hum_{21} G-quadruplex DNA in the corresponding buffer.

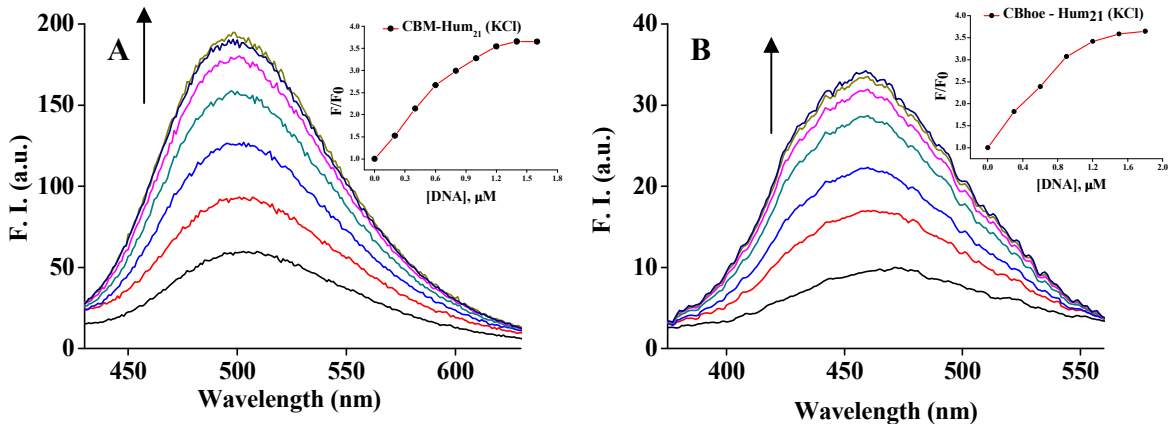

Figure S4. Fluorescence titration spectra of 0.4 μM ligand (A) **CBM** and (B) **CBhoe** in 10 mM Tris-HCl (pH 7.4), 0.1 mM EDTA and 0.1 M KCl with 10 μM pre-formed Hum_{21} G-quadruplex DNA.

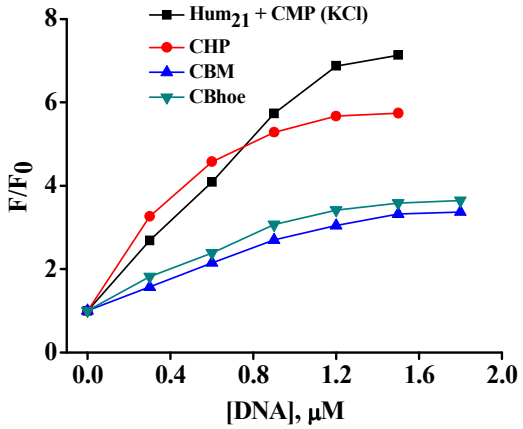

Figure S5. Relative enhancement in the fluorescence intensities of the ligands (**CMP**, **CHP**, **CBM** and **CBhoe**) in 10 mM Tris-HCl (pH 7.4), 0.1 mM EDTA and 0.1 M KCl upon interaction with the Hum_{21} G-quadruplex DNA/CT DNA.

The ligands binding affinities towards the G4 DNA have also been calculated from the fluorescence titration data (Figure S6). The dissociation constants (K_d) were found to be quite similar with that calculated from the UV-Vis titrations (Table S2). The small difference in the magnitude in K_d may be due to the difference in the experimental procedure as reported earlier.[3]

The binding affinities of the ligands with the G4 DNA were performed from the fluorescence emission studies at 20 °C using fixed ligand concentration of 400 nM and varying the G-quadruplex DNA concentration.

The binding affinity of the ligands was calculated following a reported protocol using the equation **1**.

$$\Delta F = (\Delta F_{max} / 2[L]_0)\{([L]_0 + [Q] + 1/K_a) - ([L]_0 + [Q] + 1/K_a)^2 - 4[L]_0[Q]\} \quad \text{.....(1)}$$

where $\Delta F = F - F_0$; $\Delta F_{max} = F_{max} - F_0$; F and F_0 are the initial and subsequent fluorescence intensities of the ligand (at 466 nm for **CMP** and **CHP**; 502 nm for **CBM**; and 458 nm for **CBhoe**) upon addition of the G4 DNA; K_a is the binding constant; $[L]_0$ is the total ligand concentration; $[Q]$ is the added quadruplex concentration. Dissociation constant (K_d) has been calculated from the equation, $K_d = 1/K_a$.

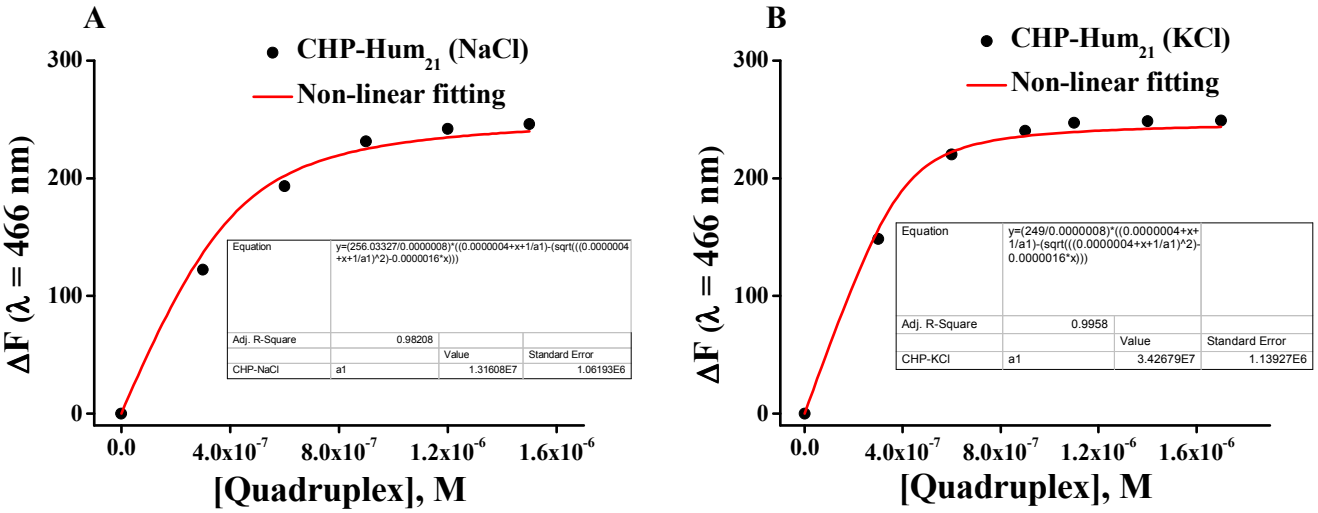

Figure S6. Determination of the binding affinities from fluorescence spectral titrations of the ligand **CHP** with the G4 DNA in (A) NaCl buffer and (B) KCl buffer.

Table S2. Dissociation constants (K_d) determined from UV-Vis absorption and fluorescence emission spectroscopy for the ligands with the pre-formed Hum_{21} G4 DNA.

Ligand	**Binding affinities determined from UV-Vis absorption titrations**[a]				**Binding affinities determined from fluorescence emission titrations**[b]	
	Hum_{21} (NaCl)		**Hum_{21} (KCl)**		**Hum_{21} (NaCl)**	**Hum_{21} (KCl)**
	K_d (μM)	n	K_d (μM)	n	K_d (μM)	K_d (μM)
CMP	0.34 ± 0.01	2.5	0.13 ± 0.01	2.7	0.15 ± 0.01	0.10 ± 0.01
CHP	0.05 ± 0.002	2.3	0.03 ± 0.002	3.2	0.08 ± 0.01	0.03 ± 0.001
CBM	0.48 ± 0.02	2.9	0.33 ± 0.04	2.6	0.19 ± 0.01	0.12 ± 0.01
CBhoe	0.38 ± 0.03	3.2	0.23 ± 0.02	3.4	0.18 ± 0.01	0.15 ± 0.01

[a]Dissociation constants (K_d) were calculated from the absorbance spectral binding assays performed with the pre-formed Hum_{21} G4 DNA in 10 mM Tris-HCl (pH 7.4) having 0.1 M NaCl/KCl and 0.1 mM EDTA. [b]Dissociation constants (K_d) were calculated from the fluorescence emission spectral binding assays performed with the pre-formed Hum_{21} G4 DNA in 10 mM Tris-HCl (pH 7.4) having 0.1 M NaCl/KCl and 0.1 mM EDTA.

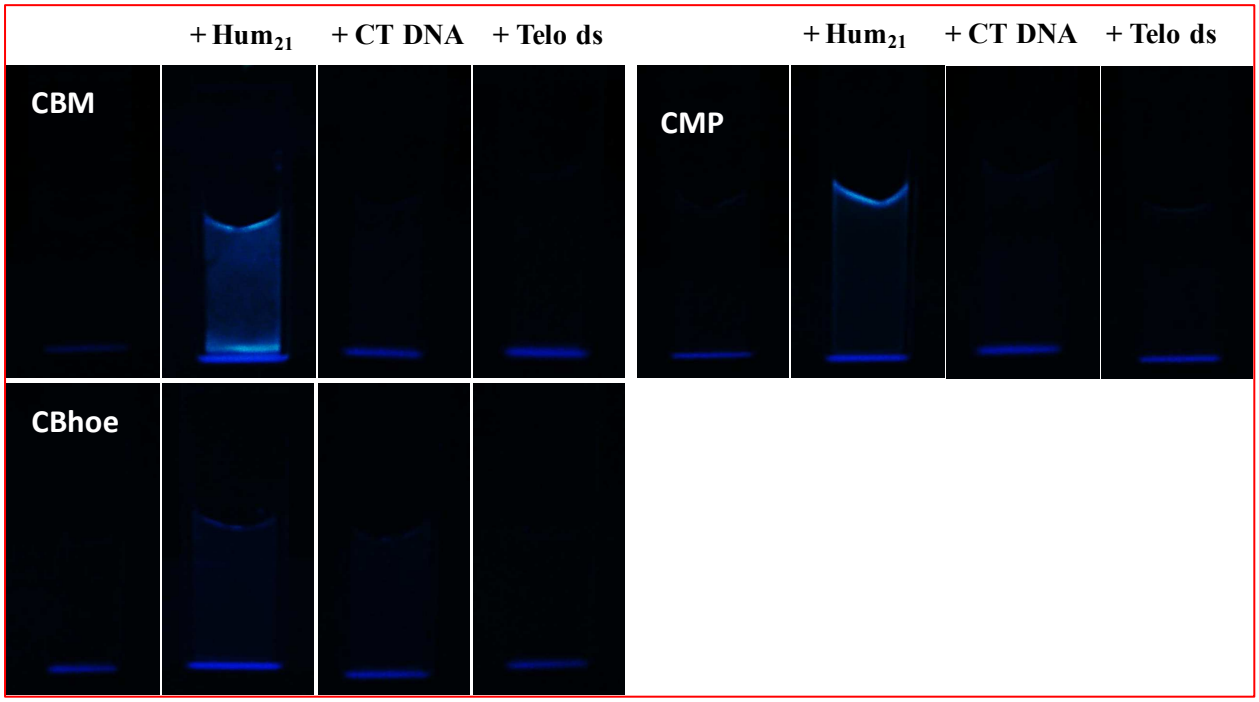

Figure S7. Fluorescence images of 20 μM ligands (**CBM**, **CMP**, and **CBhoe**) and ligand-DNA complexes (with 40 μM of Hum_{21}, CT DNA and Telo ds DNA) under UV light (λ_{ex} = 365 nm) in 10 mM Tris-HCl (pH 7.4) having 0.1 M KCl and 0.1 mM EDTA.

Additional CD titration data.

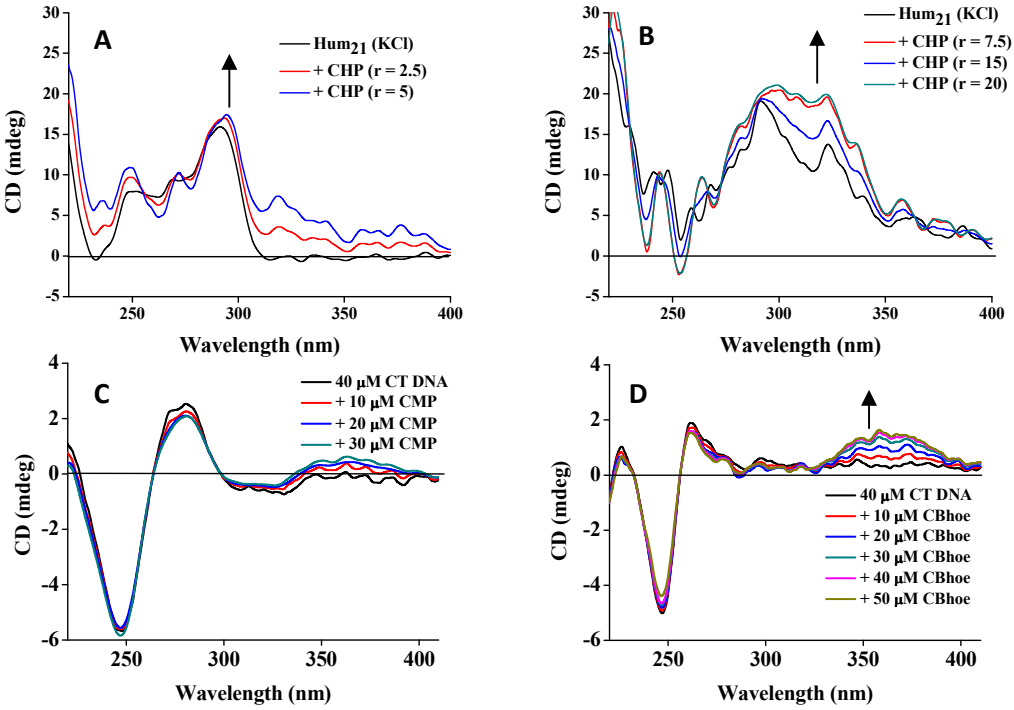

Figure S8. (A, B) CD spectral titrations of 4 µM Hum_{21} G-quadruplex DNA with increasing concentration of **CHP** in 10 mM Tris-HCl (pH 7.4) containing 0.1 mM EDTA and 0.1 M KCl. CD spectral titration of CT DNA with (C) **CMP** and (D) **CBhoe** in 10 mM Tris-HCl (pH 7.4) containing 40 mM NaCl and 0.1 mM EDTA.

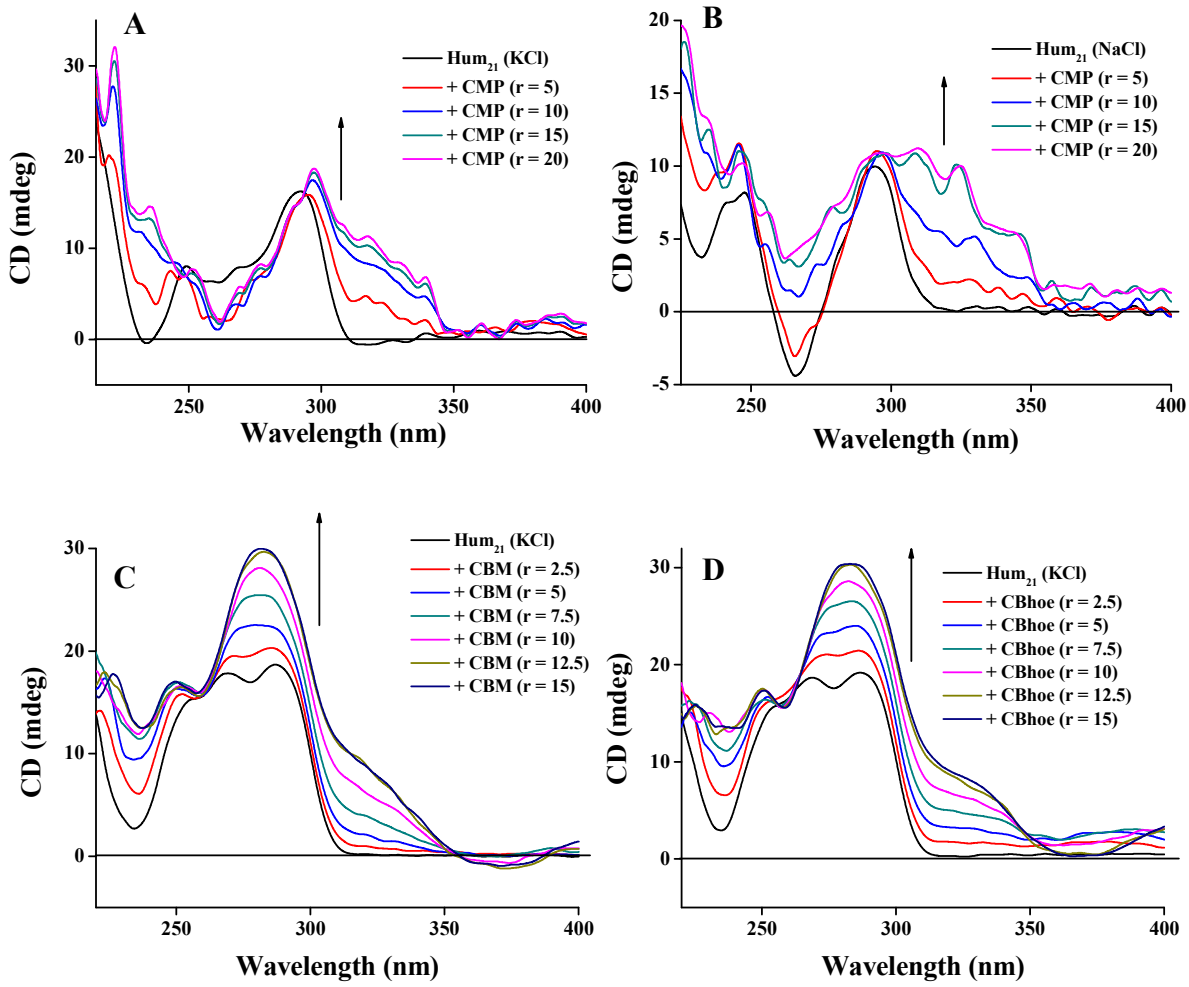

Figure S9. CD titration of 4 μM Hum_{21} G-quadruplex with **CMP** in Tris-HCl (pH 7.4), having 0.1 mM EDTA and (A) 0.1 M KCl (B) NaCl. CD titration of 4 μM Hum_{21} G-quadruplex with (C) **CBM** and (D) **CBhoe** in Tris-HCl (pH 7.4), 0.1 M KCl and 0.1 mM EDTA

Formation of G-quadruplex DNA in the presence of ligand.

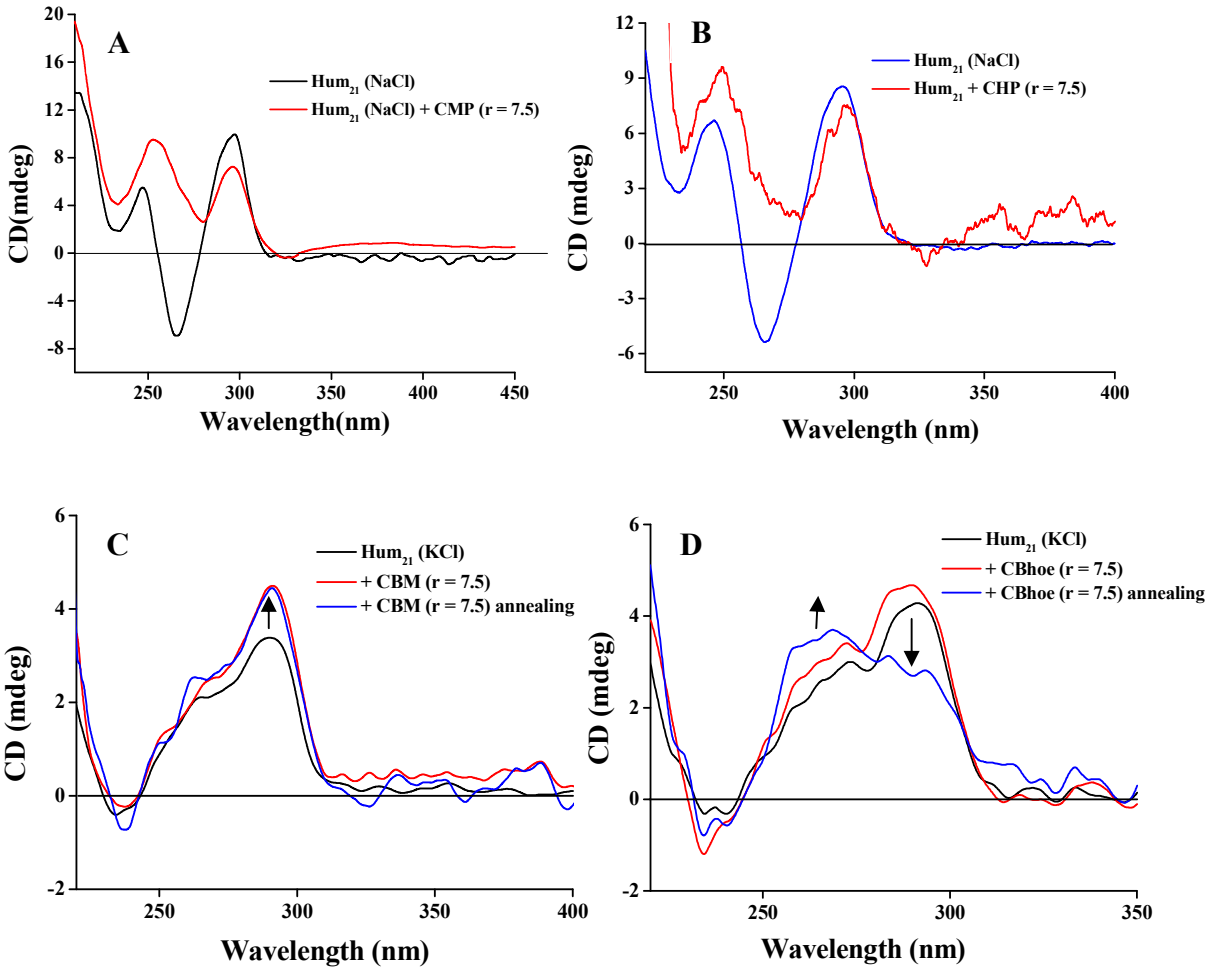

Figure S10. Formation of quadruplex in the presence of (A) **CMP** and (B) **CHP** in 10 mM Tris-HCl (pH 7.4), containing 0.1 M NaCl and 0.1 mM EDTA. Formation of quadruplex in the presence of (A) **CBM** and (B) **CBhoe** in 10 mM Tris-HCl (pH 7.4), containing 0.1 M KCl and 0.1 mM EDTA.

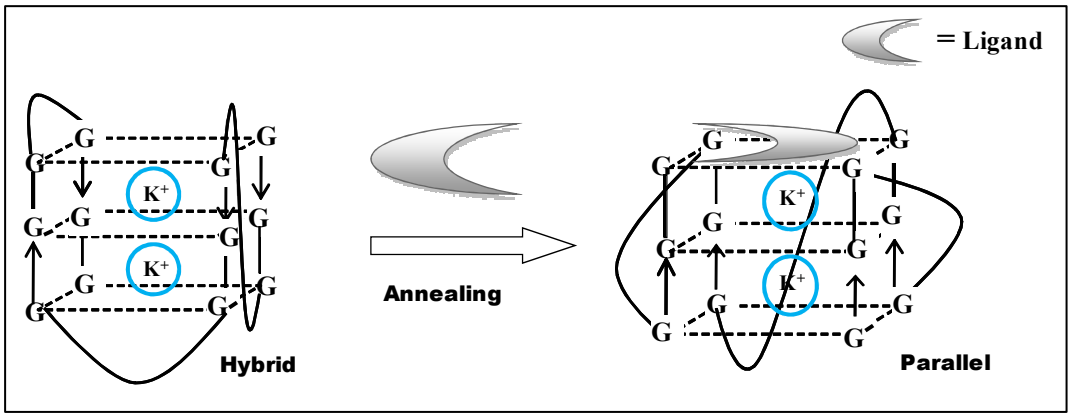

Figure S11. A schematic representation of change in the G-quadruplex DNA structure during the ligand mediated topological alteration.

Additional DNA melting experiment data.

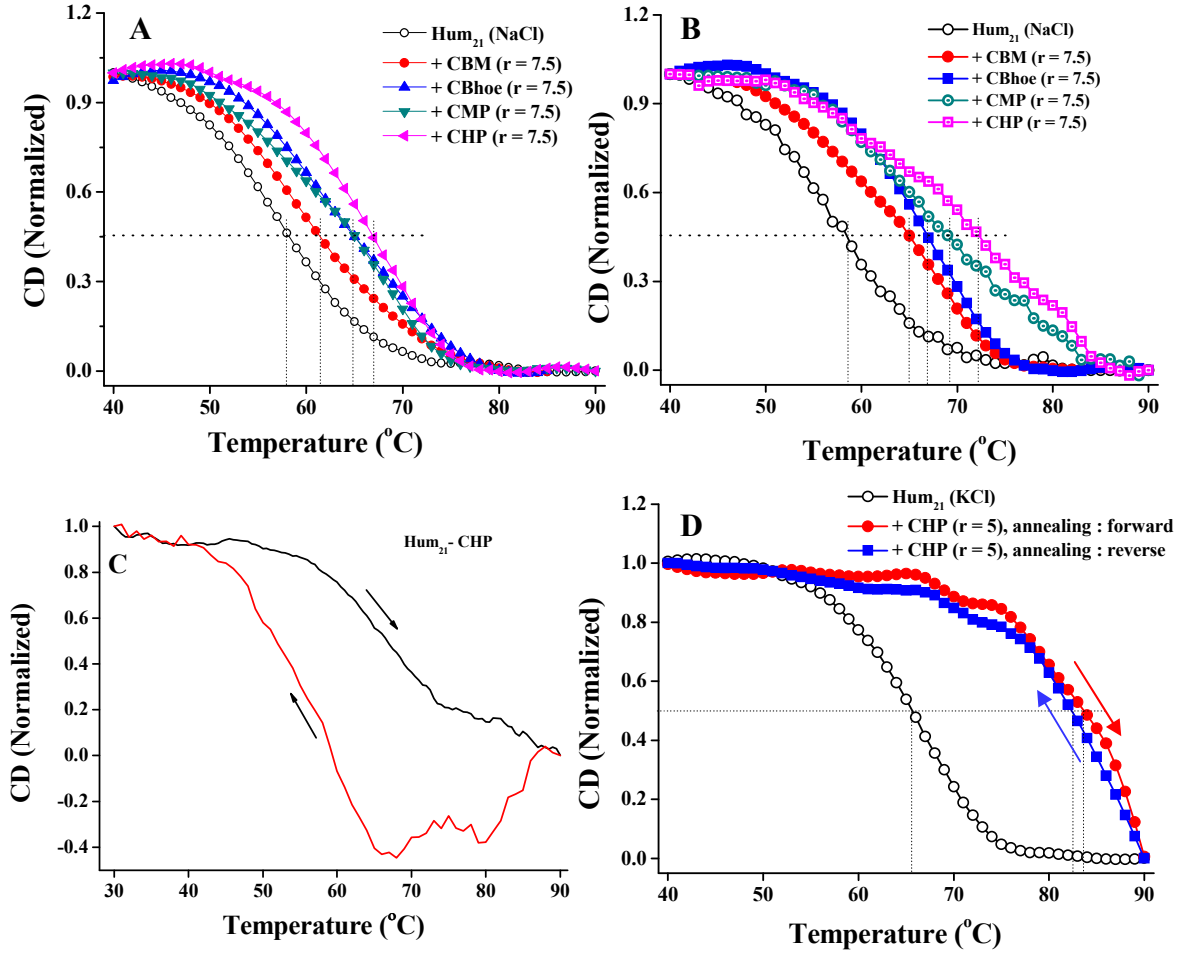

Figure S12. (A) Melting profile of the preformed quadruplex and quadruplex incubated with ligands for 12 h in specified concentration in NaCl buffer monitored at a wavelength of 295 nm. (B) Melting profile of preformed quadruplex and quadruplex formed in presence of ligands with specified concentration in NaCl buffer monitored at a wavelength of 295 nm. (C) Hysteresis in the CD melting profiles of the preformed Hum_{21} G-quadruplex DNA incubated with **CHP** (r = 7.5) in NaCl buffer monitored at a wavelength of 295 nm. (D) Melting profile of G-quadruplex DNA formed in presence of **CHP** (r = 5) in 10 mM Tris-HCl, 0.1 M KCl, 0.1 mM EDTA, pH 7.4 buffer monitored at a wavelength of 263 nm.

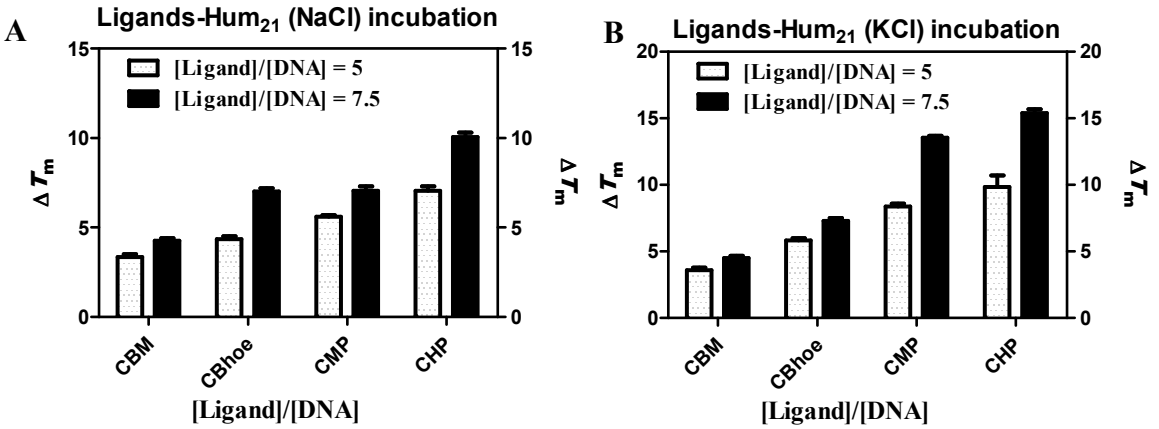

Figure S13. Plot of elevation in the denaturation temperatures of Hum_{21} G-quadruplex DNA upon specific ligand binding at different concentration in 10 mM Tris-HCl (pH 7.4) containing 0.1 mM EDTA and (A) 0.1 M NaCl or (B) 0.1 M KCl.

TRAP-LIG Assay.

A modified TRAP assay was performed using a three-step TRAP–LIG procedure.[4]

Step 1. The initial elongation process was carried out by preparing a master mix containing 0.1 μg of TS forward primer (5′-AAT CCG TCG AGC AGA GTT-3′), TRAP buffer (20 mM Tris–HCl, pH 8.3, 68 mM KCl, 1.5 mM $MgCl_2$, 1 mM EGTA, and 0.05% [v/v] Tween 20), dNTPs (125 μM each), and protein extract (500 ng/sample) diluted in CHAPS lysis buffer (10 mM Tris–HCl, pH 7.5, 1 mM $MgCl_2$, 1 mM EGTA, 0.5% CHAPS, 10% glycerol, 5 mM β-mercaptoethanol, and 0.1 mM 4-(2-aminoethyl)-benzene sulfonyl fluoride. The PCR master mix was added to each tube containing freshly prepared ligand solutions at various concentrations and to a negative control containing no ligand. The initial elongation step was first carried out at

37 °C for 30 min and then heated at 94 °C for 5 min to deactivate the telomerase and finally maintaining the mixture at 20 °C.

Step 2. The purification of the elongated product and removal of the bound and free ligands were performed using the QIA kit (Qiagen) according to the manufacturer's instructions. This kit is specially designed for the purification of both double- and single-stranded ODNs from 17 bases in length. It employs a high-salt buffer to bind the negatively charged ODNs to the positively charged spin tube membrane through centrifugation so that all the other components, including the positively charged and neutral ligand molecules, are eluted. A PCR-grade water was then used to wash any impurities away before the elution of DNA using a low-salt concentration solution. The purified samples were freeze-dried and then re-dissolved in PCR-grade water at room temperature prior to the second amplification step.

Step 3. The purified, extended samples were then subjected to PCR amplification. For this, a second PCR master mix was prepared consisting of 1 μM ACX reverse primer (5′-GCG CGG $[CTTACC]_3$ CTA ACC-3′), 0.1 μg TS forward primer (5′-AAT CCG TCG AGC AGA GTT-3′), TRAP buffer, 5 μg BSA, 0.5 mM dNTPs, and 2 U *Taq* polymerase. A 6 μl aliquot of the master mix was added to the purified telomerase extended samples and amplified for 30 cycles of: 30 s at 94 °C and 30 s at 59 °C. The reaction products were loaded onto a 10% polyacrylamide gel (19:1) in TBE 0.5 X against 1800V. Gels were then transferred to a Whatman (3 mm) paper, dried under vacuum at 80 °C, and read using a phosphorimager 840 (Amersham). Measurements were made in triplicate with respect to a negative control run using the equivalent TRAP-PCR conditions but omitting the protein extract, thus ensuring that the ladders observed were not due to the artefacts of the PCR reaction.

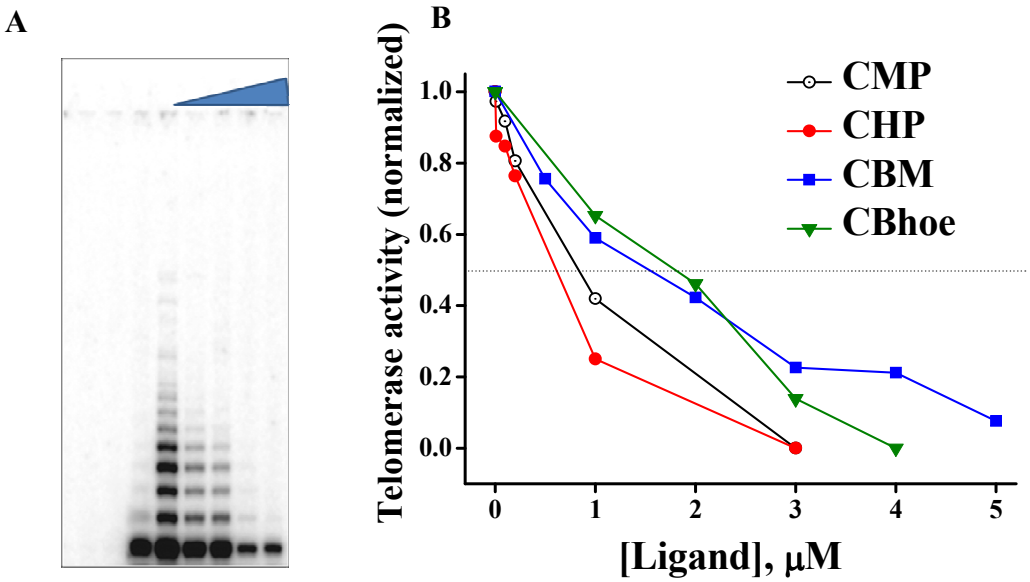

Figure S14. (A) Telomerase inhibition assay (TRAP-LIG) for ligand **CBhoe**. (B) Plot of normalized telomerase activity against added ligand concentration in TRAP-LIG assay for the calculation of IC_{50} value.

Additional cell viability assays.

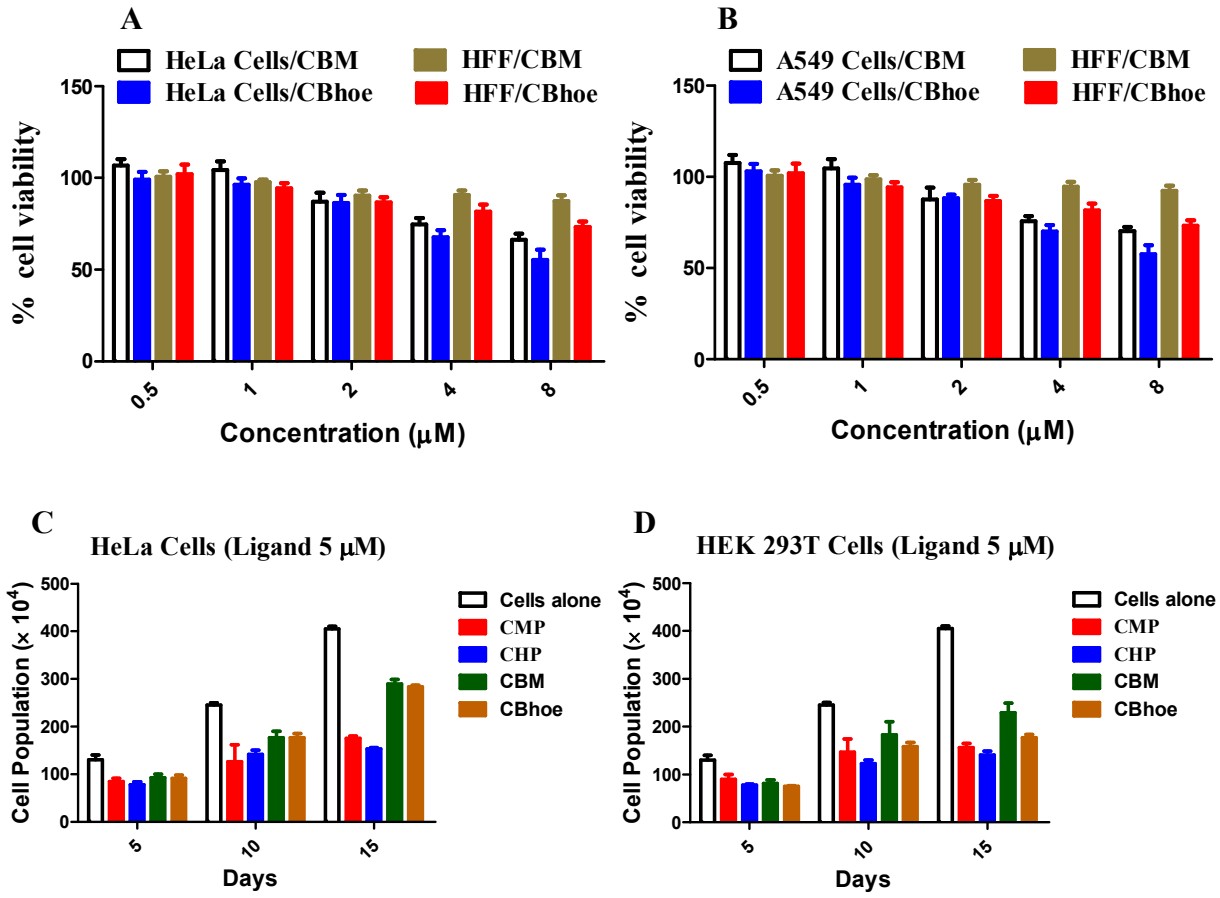

Figure S15. Effect of **CBM** and **CBhoe** on the cell viability after short-term exposure (72 h) to different cancer and normal cells, (A) HeLa cells and HFF cells; (B) A549 cells and HFF cells as measured by the MTT assays. Cells were treated with each concentration in triplicates in individual experiments and the results shown are based on at least three independent experiments. Effect of ligands (**CMP**, **CHP**, **CBM**, and **CBhoe**) on the cell viability upon long-term exposure (15 days) to (C) human cervical cancer cells (HeLa) and (D) human embryonic kidney transformed cells (HEK293T) as measured using the MTT assay.

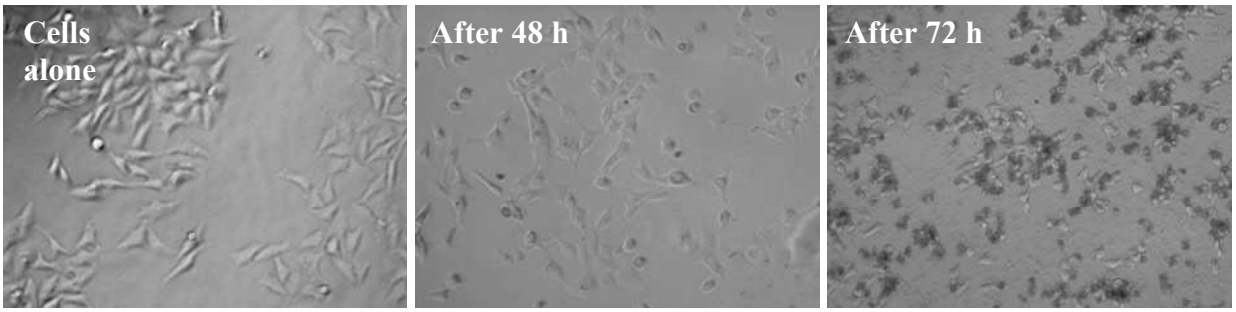

Figure 16. Representative bright field images for cell morphology of ligand treated (4 μM of **CMP**) human cervical cancer cells (HeLa) at different time intervals.

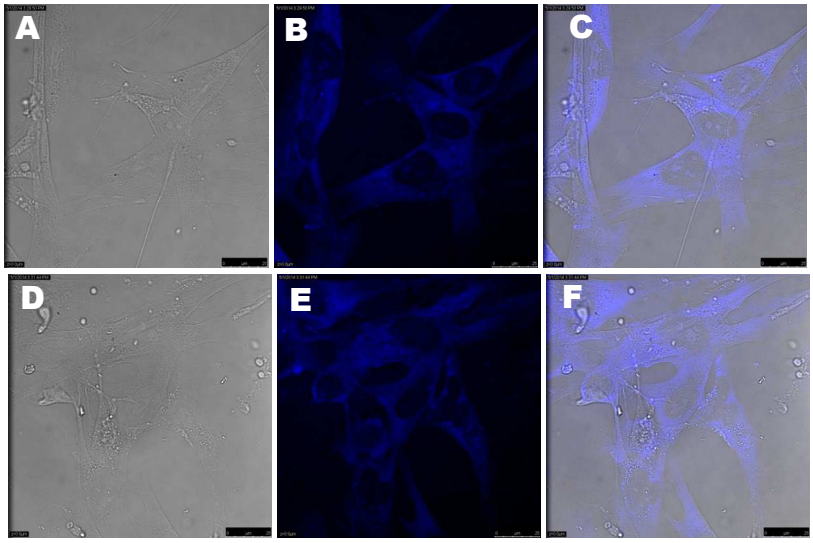

Figure S17. Representative confocal microscopic images depicting cellular internalization of ligands at a concentration of 10 μM, **CHP** (A) and **CMP** (B) for 12 h in HFF normal cells. Panels A, B and C (left to right) represent bright field, ligand fluorescence (blue) and overlay of the two respectively.

Computational Methods. The molecular energy optimization were performed using *Gaussian 03* suite program at B3LYP/6-31G* level of theory. The Mulliken atomic charges of the optimized conformation were obtained from the calculations and used for the docking studies.

The optimized structures were converted into PDB using Open Babel software. The mode of binding of each ligand molecule with the G-quadruplex DNA has been investigated by docking[5] in the primary step followed by MD simulations.[6] At the first stage the energy optimized ligand structures were docked with the parallel propeller-type G4 DNA structure as reported on the basis of single-crystal X-ray diffraction (PDB 1KF1) using *Autodock 4.0* software.[5] The 22-mer 1KF1 structure shows that it has four grooves formed by the three TTA loops along with two G-quartet surface in the 3′- and 5′-ends which offer potential targets for the ligand binding.[7] Initially blind docking was performed with a maximum grid box (126 × 126 × 126 points; spacing 0.375 Å) keeping the macromolecule at the center and static.

Docking calculations were carried out using the Lamarckian genetic algorithm (LGA). Initially, we used a population of random individuals (population size: 150), a maximum number of 2500000 energy evaluations, a maximum number of generations of 27000, and a mutation rate of 0.02. Two hundred independent docking runs were performed for each ligand. The resulting positions were ascertained according to a root-mean-square criterion of 0.5 Å. Energetically minimized as well as maximum in clustering structure (Figure S18) has been taken for the next level of theory, MD simulation.

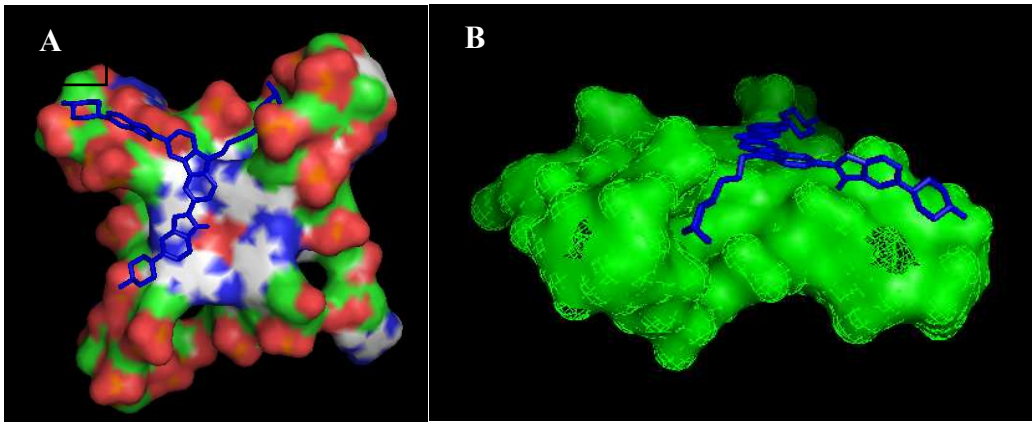

Figure S18. A top view (**A**) and side view (**B**) of the optimized ligand (**CMP**) and parallel propeller-type G-quadruplex DNA (1KF1) complex after docking in *AUTODOCK* 4.0. The ligand has been shown in 'stick' model whereas the DNA has been shown in 'surface' model and 'mesh' view in PyMOL software.

Molecular dynamics simulations were performed using the ff99bsc0 force field in the AMBER 9.0 software package with *AmberTools* 1.3.[6] Partial atomic charges for the ligand molecules were derived using the HF/6-31G* basis sets followed by RESP calculation, while the force-field parameters were taken from the generalized Amber force field (GAFF)[8] using ANTECHAMBER module. Periodic boundary conditions were applied with the particle-mesh Ewald (PME) method used to treat long-range electrostatic interactions.[9] The G-quadruplex DNA and the ligand complexes were solvated in a truncated octahedral box of TIP3P water molecules with solvent layers of 10 Å thicknesses, and the potassium counter ions were added to neutralize the complexes. The hydrogen bonds were constrained using SHAKE to illustrate the non-bonded interactions and a residue-based cut off of 10 Å was used. The solvated structures were subjected to initial 1000 steps of minimization to equilibrate the solvent and the counter

cations in two steps under force constant of 500 and 50 kcal mol^{-1}. Then the minimization was carried out for the total system without any restrain for 2500 steps. The system was then heated slowly from 0 to 300 K in a 20 ps simulation keeping the volume constant with restraints of 50 kcal mol^{-1} for the macromolecule. The temperature has been controlled using Langevin dynamics with a collision frequency of 1.0 ps^{-1} and molecular dynamic run with a time step of 2 fs per step. Then it was allowed to equilibrate keeping the pressure constant with gradual decrease of constraints (40, 30, 20, 10 kcal mol^{-1}) for 50 ps each step at a temperature of 300 K. After that 1 ns equilibration step has been carried out under minimum constraints of 5 kcal mol^{-1} followed by 6 ns final production run without any constraint. The output and trajectory files were saved in every 2 fs for the subsequent analysis respectively. All trajectory analysis were performed using the Ptraj module in the Amber 9.0 suite and examined visually using the VMD software package (Figure S19).[10]

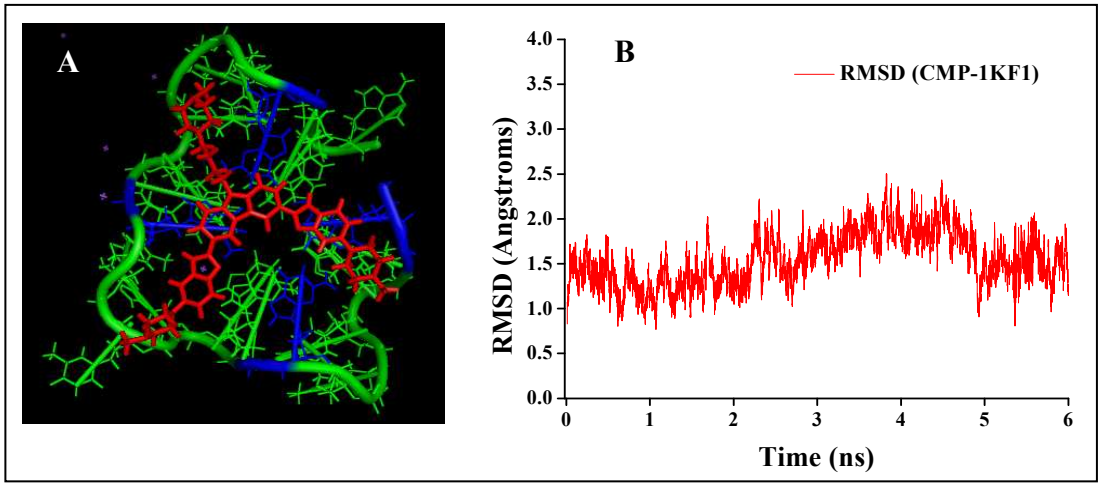

Figure S19. (A) Ligand-DNA complex structure after final MD simulation of 6 ns and (B) corresponding RMSD plot.

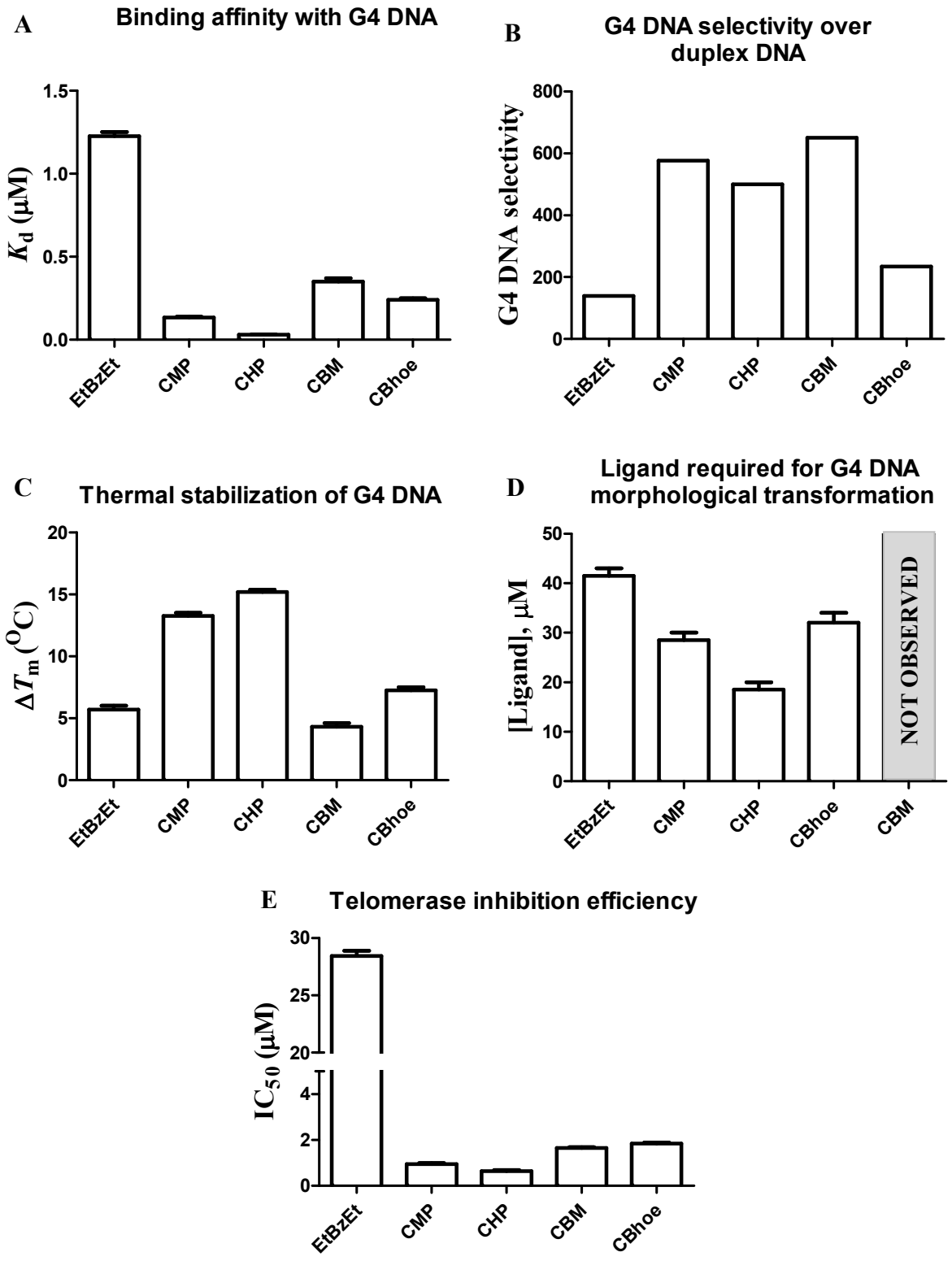

Figure S20. Graphical representation of the ligand's relative activities as obtained from different, independent experimental methods (UV-Vis spectral titrations, CD spectroscopy and TRAP-LIG assay).

References.

(1) Kelly, D. P.; Bateman, S. A.; Martin, R. F.; Reum, M. E.; Rose, M.; Whittaker, A. R. D. Synthesis and characterization of boron-containing bibenzimidazoles related to the minor groove binder, Hoechst 33258. *Aust. J. Chem.* **1994**, *47*, 247-262.

(2) Peacocke, A. R.; Skerrett, J. N. H. The interaction of aminoacridines with nucleic acids. *Faraday Trans*. **1956**, *52*, 261-279.

(3) Maiti, S.; Chaudhury, N. K.; Chowdhury, S. Hoechst 33258 binds to G-quadruplex in the promoter region of human c-myc. *Biochem. Biophys. Res. Commun*. **2003**, *310*, 505-512.

(4) (a) Reed, J.; Gunaratnam, M.; Beltran, M.; Reszka, A. P.; Vilar, R.; Neidle, S. TRAP–LIG, a modified telomere repeat amplification protocol assay to quantitate telomerase inhibition by small molecules. *Anal. Biochem*. **2008**, *380*, 99-105. (b) De Cian, A.; Cristofari, G.; Reichenbach, P.; De Lemos, E.; Monchaud, D.; Teulade-Fichou, M. P.; Shin-Ya, K.; Lacroix, L.; Lingner, J.; Mergny, J. L. Reevaluation of telomerase inhibition by quadruplex ligands and their mechanisms of action. *Proc. Natl. Acad. Sci.* **2007**, *104*, 17347-17352.

(5) Morris, G. M.; Goodsell, D. S.; Halliday, R. S.; Huey, R.; Hart, W. E.; Belew, R. K.; Olson, A. J. *J. Comput. Chem.* **1998**, *19*, 1639-1662.

(6) Case, D. A.; Cheatham, T.; Darden, T.; Gohlke, H.; Luo, R.; Merz, K. M.; Onufriev, A. Jr.; Simmerling, C.; Wang, B.; Woods, R. The amber biomolecular simulation programs. *J. Computat. Chem.* **2005**, *26***,** 1668-1688.

(7) (a) Han, H.; Hurley, L. H. G-quadruplex DNA: a potential target for anticancer drug design. *Trends Pharmacol. Sci.* **2000**, *21*, 136-142. (b) Cian, A. D.; DeLemos, E.; Mergny, J-L.; Teulade-Fichou, M-P.; Monchaud, D. Highly efficient G-quadruplex recognition by bisquinolinium compounds. *J. Am. Chem. Soc.* **2007**, *129*, 1856-1857. (c) Ou, T-M.; Lu, Y-J.;

Zhang, C.; Huang, Z-S.; Wang, X-D.; Tan, J-H.; Chen, Y.; Ma, D-L.; Wong, K-Y.; Tang, J. C-O.; Chan, A. S-C.; Gu, L-Q. Stabilization of G-quadruplex DNA and down-regulation of oncogene *c-myc* by quindoline derivatives. *J. Med. Chem.* **2007**, *50,* 1465-1474.

(8) Wang, J.; Wolf, R. M.; Caldwell, J. W.; Kollman, P. A.; Case, D. A. Development and testing of a general amber force field. *J. Comput. Chem.* **2004** *25*, 1157-1174.

(11) Darden, T.; York, D.; Pedersen, L. Particle mesh Ewald: An *N* -log(N) method for Ewald sums in large systems. *J. Chem. Phys.* **1993**, *98*, 10089-10092.

(12) Humphrey, W.; Dalke, A.; Schulten, K. VMD: Visual molecular dynamics. *J. Mol. Graph.***1996**, *14*, 33-38.

Table S3. Elemental Analysis Data for the Compounds **CMP** , **CHP**, **CBM**, and **CBhoe**.

Compound	% of elements (Calculated)	% of elements (Found)
CMP	(calcd. for $C_{45}H_{55}N_{11}.0.5H_2O$): C, 71.21; H, 7.44 N, 20.30.	C, 71.42; H, 7.40; N, 20.27.
CHP	(calcd. for $C_{47}H_{59}N_{11}O_{2)}$: C, 69.69; H, 7.34; N, 19.02	C, 69.42; H, 7.40; N, 19.08
CBM	(calcd. for $C_{43}H_{49}N_9O_2$): C, 71.34; H, 6.82; N, 17.4.	C, 71.82; H, 6.76; N, 17.28.
CBhoe	(calcd. for $C_{59}H_{63}N_{15}$): C, 72.15; H, 6.46; N, 21.39.	C, 71.98; H, 6.41; N, 21.48.

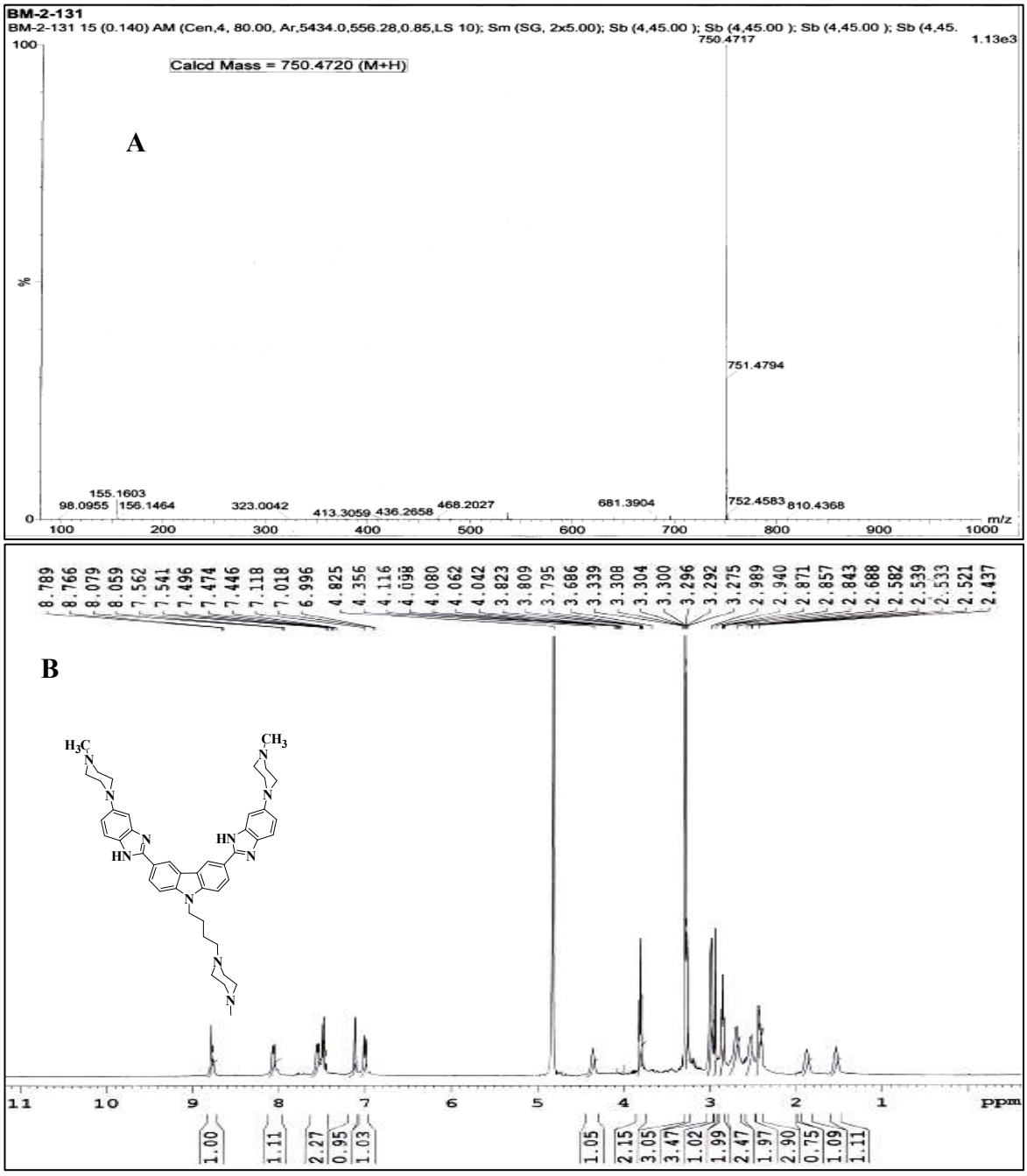

Figure S21. (A) Mass spectrum (B) ^{1}H NMR spectrum of **CMP**.

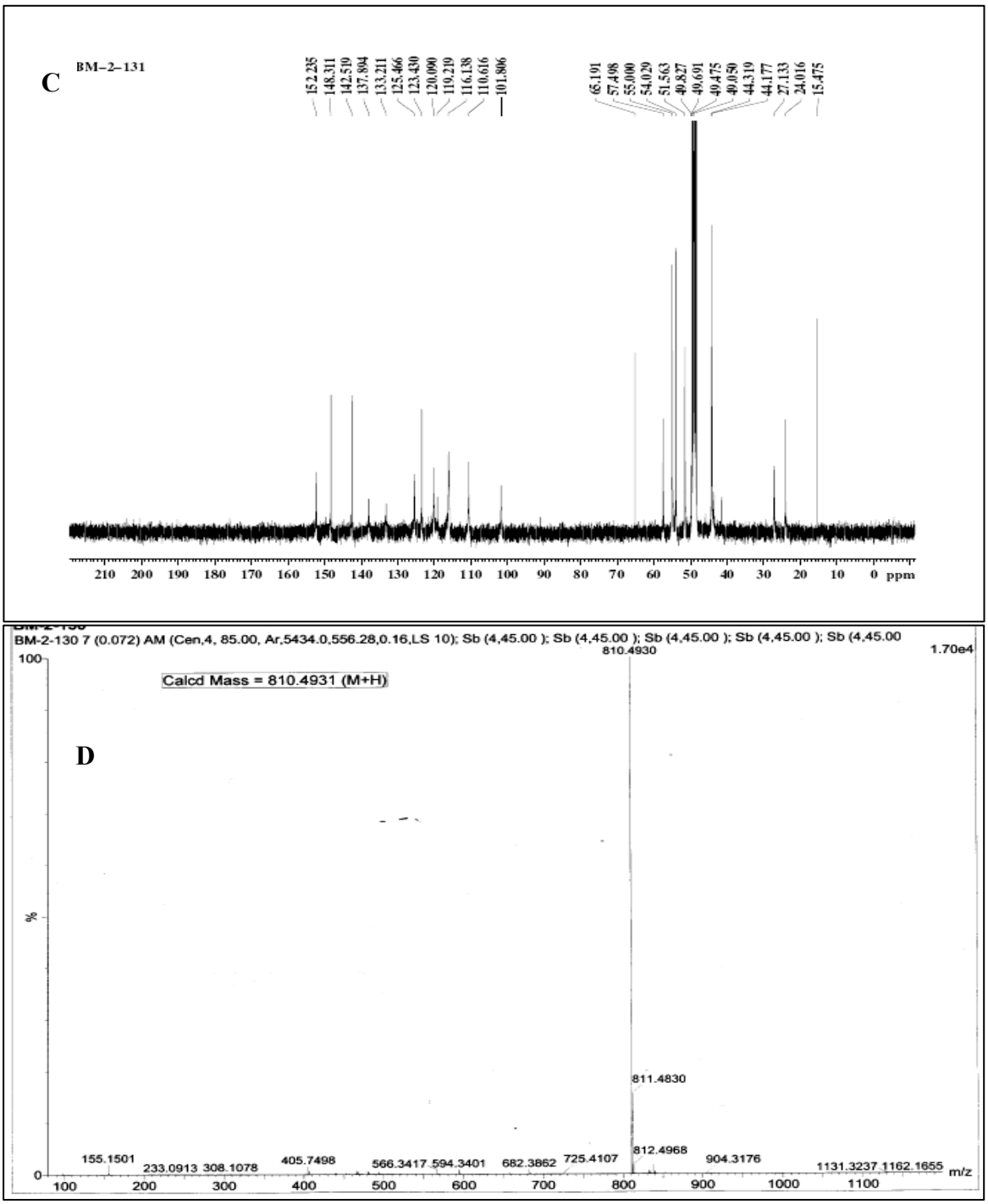

Figure S22. (A) ^{13}C NMR spectrum of **CMP** and (D) Mass spectrum of **CHP**.

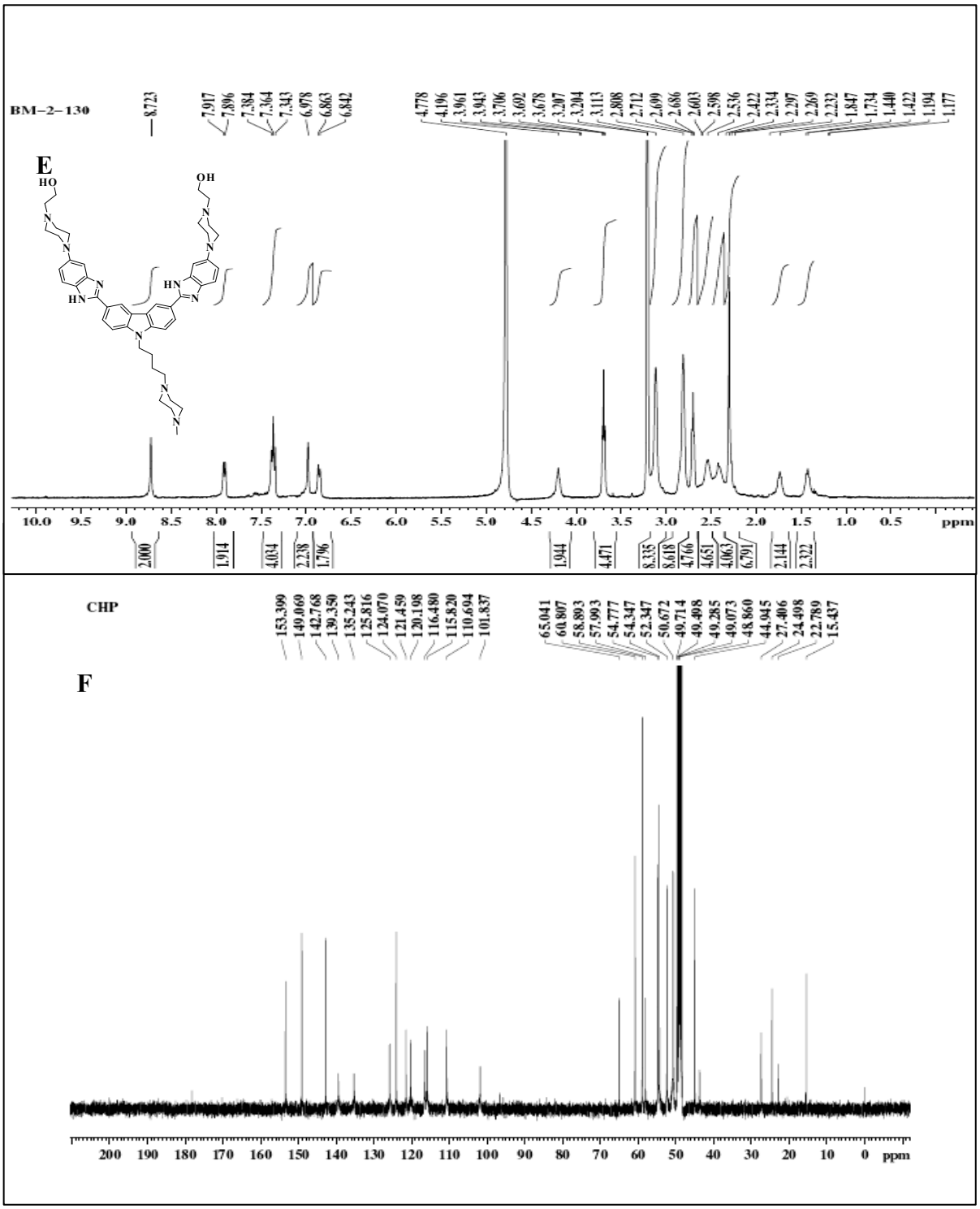

Figure S23 . (E) ^{1}H NMR spectrum of **CHP** and (F) ^{13}C NMR spectrum of **CHP**.

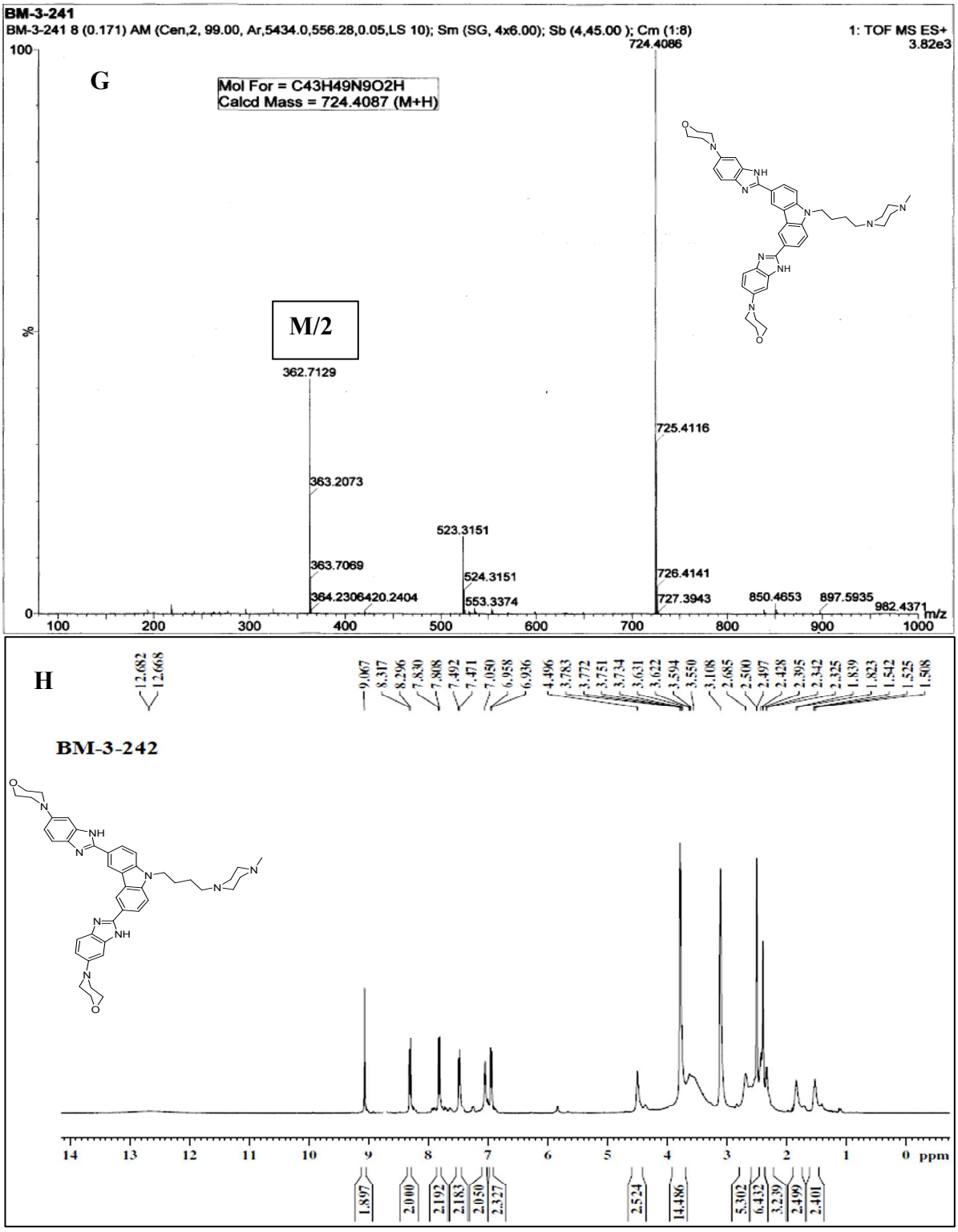

Figure S24 . (G) Mass and (H) ^{1}H NMR spectra of **CBM**.

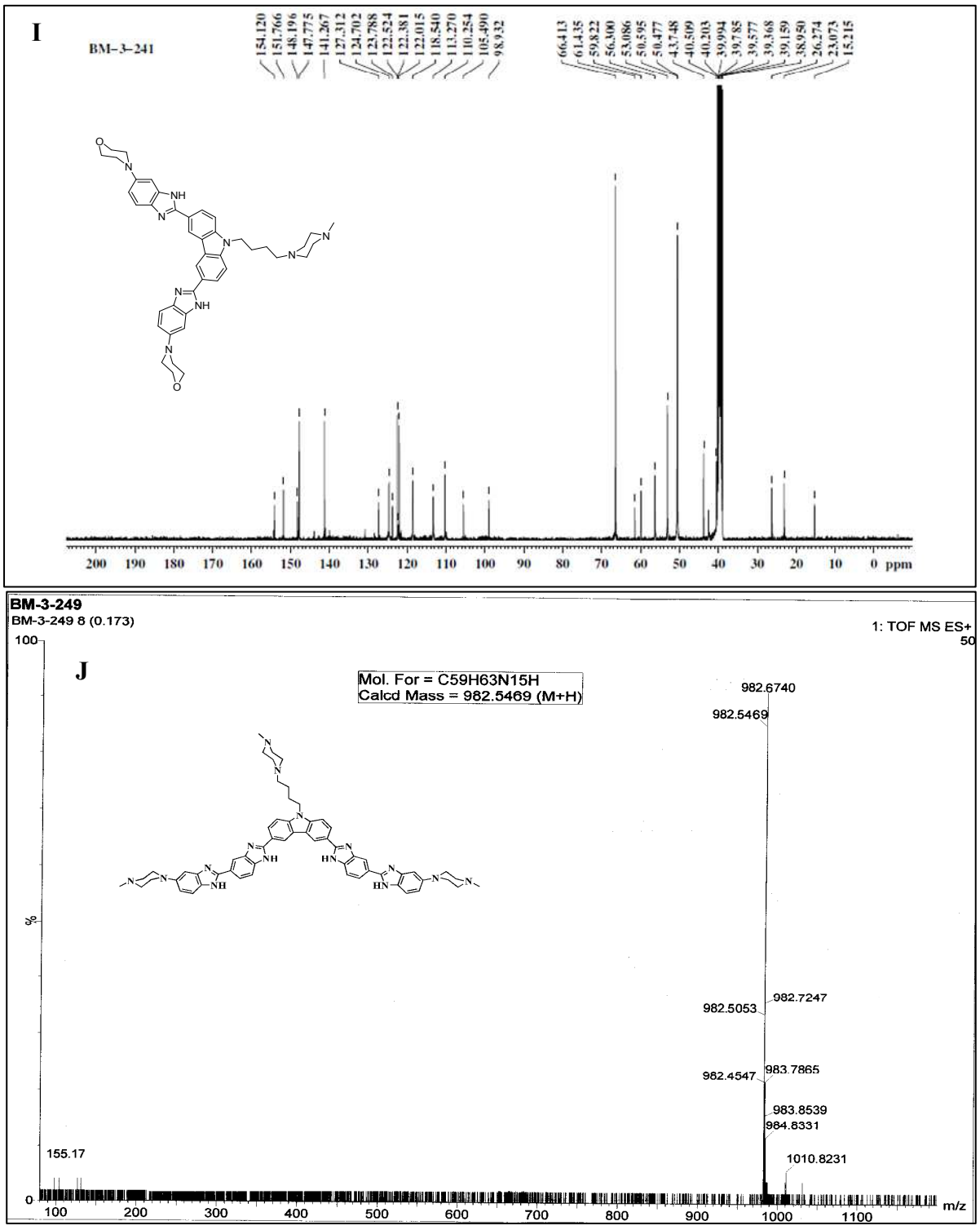

Figure S25. (I) ^{13}C NMR spectrum of **CBM** and (J) Mass spectrum of **CBhoe**.

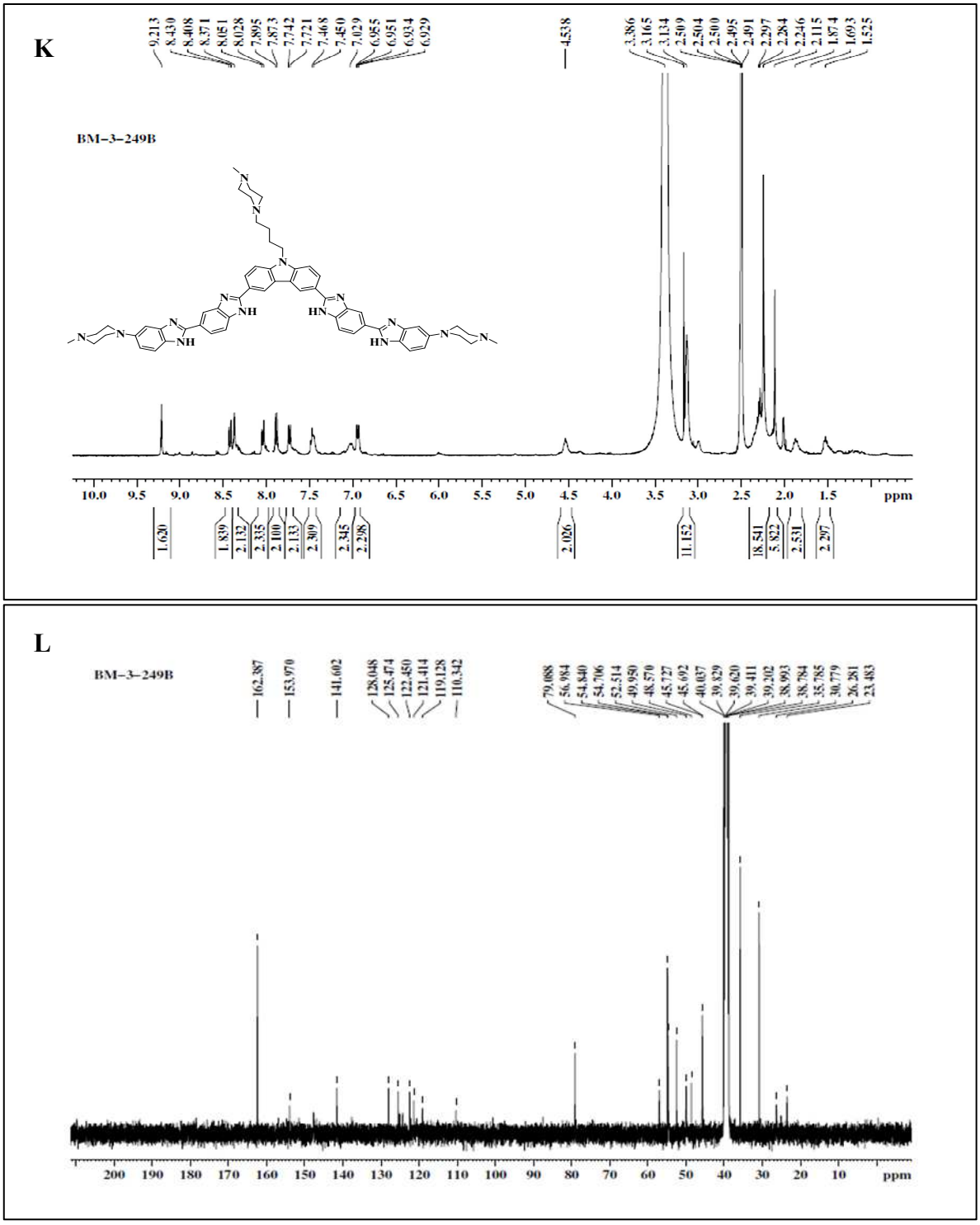

Figure S26. (K) ^{1}H NMR spectrum of **CBhoe** and (L) ^{13}C NMR spectrum of **CBhoe**.

Determination of p*K*a of the ligands.

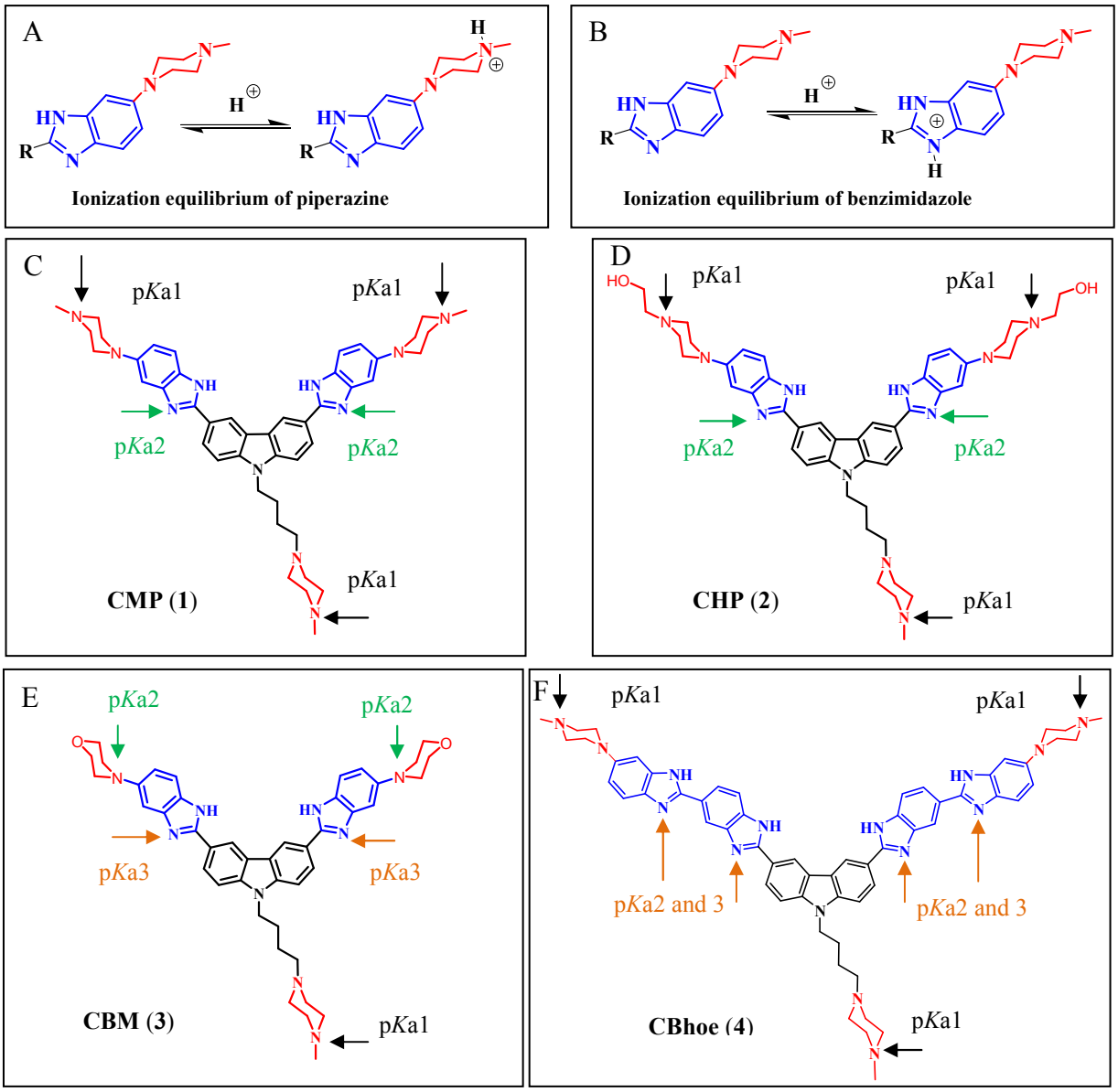

Figure S27. (A, B) Schematic representation of protonation-deprotonation equilibrium of piperazine and benzimidazole moieties present in the ligand structure. (C-F) Molecular structures of the ligands (**1-4**) depicting various protonatable sites at different pH of the medium corresponding to their p*K*a.

Table S4. p*K*a values of ligands **CMP**, **CHP**, **CBM** and **CBhoe** determined by UV-Vis spectroscopy.

Ligand	**p*K*a1**	**p*K*a2**	**p*K*a3**
CMP	8.7-7.5	6.0-4.4	
CHP	8.9-8.1	4.6-3.3	
CBM	8.1	7.3-7.1	4.9-3.3
CBhoe	7.9-7.3	6.6-5.5	4.2-3.1